논문 2004-41SD-7-6

임플랜트 및 금속전극 반경에 따른 임플랜트 VCSEL 정특성의 변화

(Tailoring the Static Characteristics of Implanted VCSELs with the Implant and Metal Aperture Radii)

김 태 용*, 김 상 배**, 최 번 재***, 손 정 환****

(Tae-Yong Kim, Sang-Bae Kim, Bun-Jae Choi, and Jeong-Hwan Son)

요 약

We have formulated an empirical analytic model for the static characteristics of implanted vertical-cavity surface-emitting lasers (VCSELs). Specifically, we have derived analytic formulas for the threshold current, slope efficiency, dynamic resistance, and the output power and forward voltage at the operation current of 12 mA in terms of the implant and metal-aperture radii by fitting the measured results. The radii of the metal aperture and implant mask of the 850 nm VCSELs range from 4 to 12.5 μm and 7 to 17.5 μm, respectively. The model shows the way of tailoring the VCSEL characteristics by changing the mask dimensions only.

Abstract

We have formulated an empirical analytic model for the static characteristics of implanted vertical-cavity surface-emitting lasers (VCSELs). Specifically, we have derived analytic formulas for the threshold current, slope efficiency, dynamic resistance, and the output power and forward voltage at the operation current of 12 mA in terms of the implant and metal-aperture radii by fitting the measured results. The radii of the metal aperture and implant mask of the 850 nm VCSELs range from 4 to 12.5 μm and 7 to 17.5 μm, respectively. The model shows the way of tailoring the VCSEL characteristics by changing the mask dimensions only.

Keywords : VCSELs, diode lasers, surface-emitting lasers

I. INTRODUCTION

VCSELs are light sources of choice in optical local area networks and interconnections, because they are considered an ideal light source for those applications. Some distinct advantages include low threshold current, suitability for 1- and 2-dimensional arrays and mass production, high reliability, low temperature dependence, and high-speed modulation capability. These excellent characteristics make VCSELs very attractive in wide variety of applications beyond the communication use, and required VCSEL charac-teristics vary widely depending on applications. Redesigning the VCSEL wafer structure is a direct approach to meet the specific requirements, but implanted-VCSEL characteristics strongly depend also on the radii of the implant mask and metal aperture [1].

Therefore, more convenient and practical approach is to change the radii of the implant mask and metal aperture while keeping the wafer structure unchanged. Nevertheless, there have been little theoretical or

* 학생회원, **정회원, 아주대학교 대학원 전자공학과
(School of Electrical and Computer Engineering, Ajou University)
*** 정회원, (주)옵토웨이
(Optoway Inc.)
**** 정회원, (주)옵토웨이퍼테크
(PROWTech Inc.)
접수일자: 2003년12월4일, 수정완료일: 2004년6월2일

experimental works relating the VCSEL characteristics to the radii. Our objective is to present an analytic easy-to-use model that relates the measured static characteristics to the radii. With the model, we can tailor the implanted-VCSEL characteristics by chang -ing only the metal aperture and implant mask radii.

II. DEVICE STRUCTURE

A cross-sectional view of the implanted VCSEL structure is depicted in Fig. 1. Adopted is a 1-λ cavity structure that contains the active layers consisting of three GaAs quantum wells. The cavity is bounded by two distributed Bragg reflector (DBR) mirrors. The upper p-type mirror is comprised of 21.5 periods of the $Al_{0.15}Ga_{0.85}As/Al_{0.95}Ga_{0.05}As$ layer pair, while the lower n-type mirror is comprised of 39 periods. All the interfaces of the mirror layers are compositionally graded to minimize the series resistance. Also, on thetop of the p-DBR is a highly doped p-type GaAs layer for a low resistance Ohmic contact. Contact metals are Au/Zn and Au/Ge/Ni for p- and n-type Ohmic contacts, respectively. All the VCSEL samples tested and modeled have the same layer structure, and only the implant mask and p-metal aperture radii differ from sample to sample. The metal aperture radius is changed from 4 to 12.5 μm, and the implant mask radius is changed from 7 to 17.5 μm. Thus, total 41 kinds of devices have been measured and modeled. Each experimental datum is obtained by taking the corresponding average value of 5 devices with the same radius combination at 23 °C.

III. MODELING THE STATIC HARACTERISTICS

Figure 2 shows the threshold current I_{th} [mA] as a function of the implant radius $r_{implant}$ [μm]. The measured threshold currents depend solely on the implant mask radius, and can be fitted to the following formula.

$$I_{th} = \pi \cdot r_{implant}^2 \cdot N_W \cdot J_{tr} \exp(g_{th}/g_0) \cdot 10^{-5} \cdot + \left(0.15 + 0.04 r_{implant} + 5/r^2_{implant}\right) [\text{mA}] \quad (1)$$

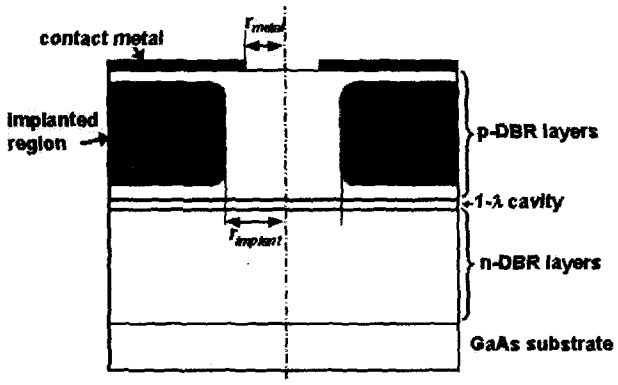

그림 1. 임플랜트 구조 수직공진 반도체 레이저의 단면도
Fig. 1. Cross-sectional structure of the implanted VCSEL

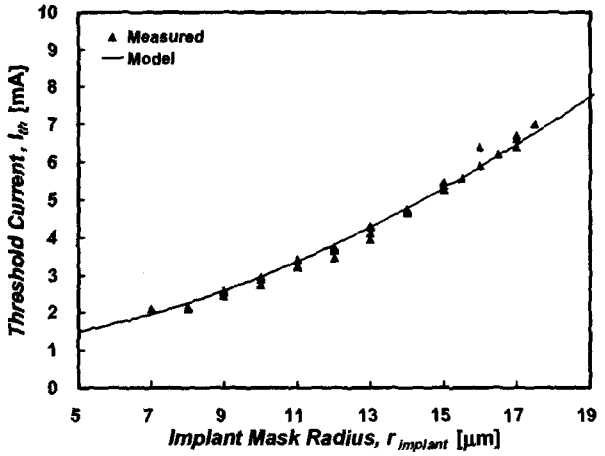

그림 2. 임플랜트 마스크 반지름과 금속전극 반지름에 따른 문턱전류의 변화. 실선은 모델링된 문턱전류를 나타내고, 점들은 23 °C에서 측정된 문턱전류
Fig. 2. The threshold current I_{th} as a function of the implant mask radius $r_{implant}$ with the metal aperture radius r_{metal} as a parameter. The solid line denotes modeled threshold current while the dots denote the threshold currents measured at 23 °C.

where N_W, J_{tr}, g_{th}, and g_0 are the number of quantum wells, transparency current density, threshold gain, and gain constant, respectively. We used 110 A/cm^2 for J_{tr} and 1300 cm^{-1} for g_0 [2], and $r_{implant}$ is in μm unit. The first term is the radiative current for lasing, and the second term is the leakage current through the p-DBR layers just below the implanted region. From the independence of I_{th} on the metal aperture radius r_{metal}, the threshold gain g_{th} is determined as $g_{th,1D}(1+15/r_{implant})$ independent of r_{metal}. The one dimensional threshold gain $g_{th,1D}$ of 459.34

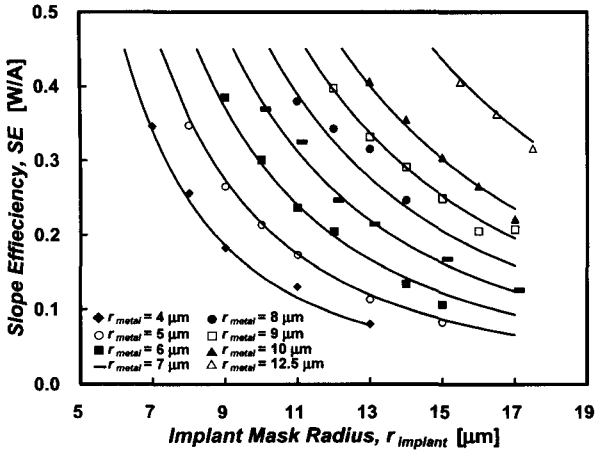

그림 3. 임플랜트 마스크 반지름과 금속전극 반지름의 조합에 따른 평균변환효율의 변화. 실선은 식 (3)으로부터 계산되어 모델링된 평균변환효율을 나타내고, 점들은 23 °C에서 측정된 평균변환효율 값

Fig. 3. The average slope efficiency for various combina-tions of the implant mask and metal aperture radii. The solid lines denote modeled values calculated from (3), and the points denote the measured ones at 23 °C.

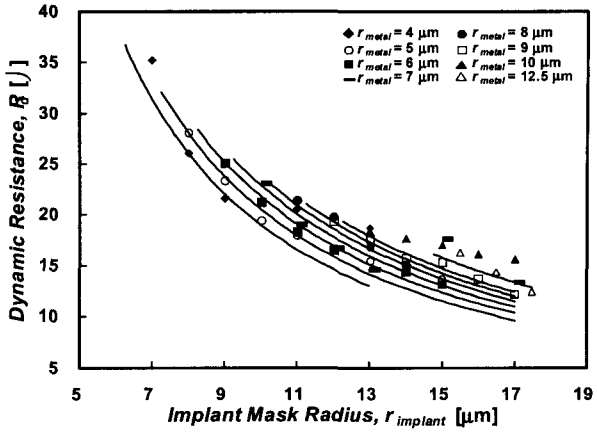

그림 4. 동저항의 임플랜트 마스크 반지름 및 금속전극 반지름 의존성. 실선은 식 (4)로부터 계산된 값이며 점들은 12 mA의 동작전류에서 측정된 동저항

Fig. 4. Dependence of the dynamic resistance on the implant mask and metal aperture radii. The solid lines denote modeled values calculated from (4) while the points denote the measured ones at the driving current of 12 mA.

cm^{-1} is calculated by a transfer matrix method for our wafer. The leakage current is calculated by the method in reference [3], and is fitted in the polynomial form in equation (1).

Figure 3 shows the average slope efficiency *SE* of the VCSELs as a function of the implant radius and the metal aperture radius. Although the linearity of the output power-driving current characteristics is good, we use the average slope efficiency defined as

$$SE = P_{op}/(I_{op} - I_{th}) \tag{2}$$

where the operation current I_{op} is set to 12 mA, and operation power P_{op} is the output power at 12 mA. The slope efficiency is expected to be a very complicated function of the VCSEL layer structure, its optical properties, optical properties of the implanted region, metal aperture radius, implant mask radius, and field profile of the various laser modes and so the driving current. But, by defining an effective implant radius and effective aperture factor, a simple formula for the slope efficiency has been derived as

$$SE = 0.90\left(\sqrt{\Gamma^2 + 0.745^2} - 0.745\right)\text{[W/A]}, \tag{3}$$

where the effective aperture factor is defined as r_{metal}/r_{eff}, and the effective implant radius r_{eff} as $r_{implant}$ 2.23 all in μm unit. The measured data and the unexpectedly simple model of (3) agree well as shown in Fig. 3. The slope efficiency for r_{metal}/r_{eff}, =1 is 0.729 [W/A], which corresponds to the measured slope efficiency of oxide-VCSELs with a similar layer structure. It is interesting that 2.23 μm in the effective implant aperture is approximately the lateral straggle of the implanted ions.

Figure 4 shows the dynamic resistance at the operation current of 12 mA for various radii com-binations. As compared to conventional edge-emitting lasers, one of the weakest points of VCSELs is their high series resistance, and the resultant heating severely limits the maximum output power even with their low temperature sensitivity. The dynamic resistance was shown to have two components: the lateral component inversely proportional to the implant radius and the vertical component inversely propor-tional to the area of the implant radius[1]. Based on this, with the metal aperture dependence newly added, we have fitted the dynamic resistance R_d as follows.

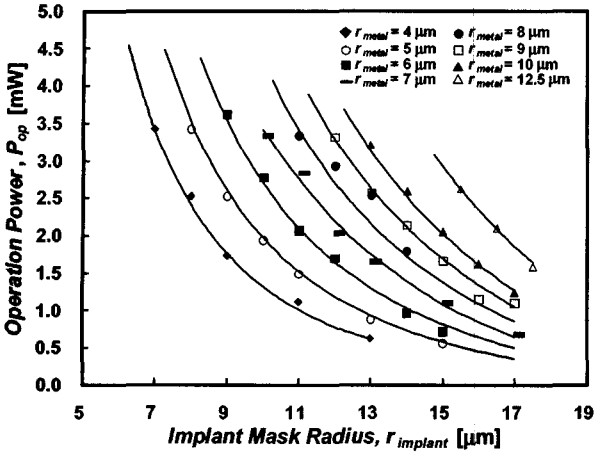

그림 5. 임플랜트 마스크 반지름 및 금속전극 반지름의 조합에 따른 광출력의 변화. 실선은 식 (5)에 의하여 계산된 값이고 점 들은 12 mA의 동작전류에서 측정된 광출력

Fig. 5. The operation power for various combinations of the implant mask and metal aperture radii. The solid lines denote modeled operation power given by (5), and the points represent the measured values at the driving current of 12 mA.

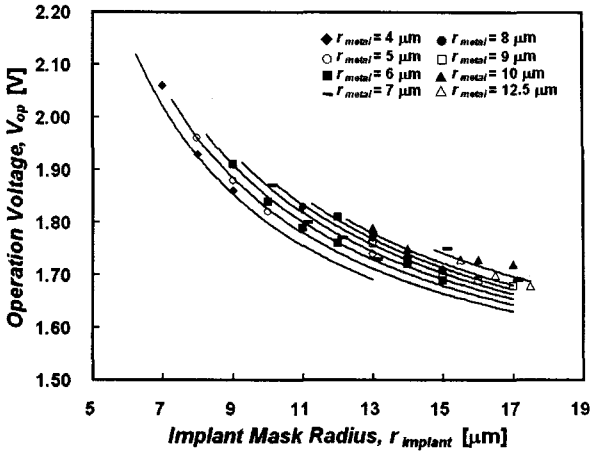

그림 6. 임플랜트 마스크 반지름 및 금속전극 반지름의 조합에 따른 동작전압의 변화. 실선은 식 (6)에 의하여 계산된 값이고 점들은 12 mA의 동작전류에서 측정된 동작전압.

Fig. 6. The operation voltage for various combinations of the implant mask and metal aperture radii. The solid lines denote modeled operation voltage given by (6) while the points represent the measured ones at the driving current of 12 mA.

$$R_d = \frac{75}{r_{implant}} \cdot \ln\left(1+\frac{24r_{metal}}{r_{implant}}\right) + \frac{125}{r_{implant}^2} \ [\Omega] \qquad (4)$$

The first term is the lateral component proportional to $1/r_{implant}$, and the second term is the vertical component proportional to $1/r^2_{implant}$. Measured dyna -mic resistance data are in good agreement with the model equation (4), as can be seen in Fig. 4.

From the users' view point, the operation power and voltage can be more meaningful, and formulas for the operation power and voltage of the VCSELs are obtained. The operation power can be extracted from the slope efficiency by using (2) and (3), and has the following form:

$$P_{op} = 0.90\left(\sqrt{\Gamma^2+0.745^2}-0.745\right)\cdot\left(I_{op}-I_{th}\right) \ [\text{mW}]. \qquad (5)$$

Figure 5 shows both the measured and modeled operation power at 12 mA for various radius combinations. An expression for the operation voltage can be derived from the dynamic resistance given by (4) with the junction voltage added. The junction voltage of our VCSELs is 1.46 V, which is given by the quasi-Fermi level separation at the lasing threshold. Thus, the operation voltage is given as

$$V_{op} = \frac{1.35}{r_{implant}} \cdot \ln\left(1+\frac{24r_{metal}}{r_{implant}}\right) + \frac{2.25}{r_{implant}^2} + 1.46 \ [\text{V}]. \qquad (6)$$

As shown in Fig. 6, fitted operation voltage is in good agreement with measured data.

IV. CONCLUSION

We have presented an experimental model for the most important static characteristics of implanted 850 nm VCSELs. The threshold current, slope efficiency, dynamic resistance, operation power and voltage have been related to the implant mask and metal aperture radii in simple analytic forms that are in good agreement with the measured results. The threshold current is shown to depend solely on the implant radius, while the slope efficiency depends on the newly defined effective aperture factor. This model enables us to tailor the VCSEL characteristics by changing only the post-epitaxy process parameters: the implant mask and metal aperture radii.

REFERENCES

[1] K. L. Lear, S. P. Kilcoyne, and S. A. Chalmers, "High power conversion efficiencies and scaling issues for vertical-cavity top-surface-emitting lasers," *IEEE Photon. Technol. Lett.*, vol. 6, no. 7, pp.778-781, July 1994.
[2] L. A. Coldren, and S. W. Corzine, 'Diode lasers and photonic integrated circuits' (John Wiley and Sons, New York, 1995) p. 173
[3] E. R. Hegblom, N. M.Margalit, B. J. Thibeault, L. A. Coldren, and J. E. Bowers, "Current spreading in apertured vertical cavity lasers", Proc. Of SPIE, vol. 3003, 1997 (San Jose), pp. 176-180

저 자 소 개

김 태 용(학생회원)
2001년 아주대학교 정보통신대학 전자공학부 졸업 (공학사)
2003년 아주대학교 대학원 전자공학과 (공학석사)
2003년 3월~ 현재 아주대학교 대학원 전자공학과 박사 과정 재학중
<주관심분야: 화합물반도체 광전소자, VCSEL>

김 상 배(정회원)
제37권 SD편 제8호 참조
현재 아주대학교 정보통신대학 전자공학부 교수
<주관심분야: 광전소자, 광전집적회로, 광통신>

최 번 재(정회원)
현재 Optoway 주임 연구원
<주관심분야: GaN LED, UV detector>

손 정 환(정회원)
1988년 서강대학교 전자공학과 학사
1990년 KAIST 전기및 전자공학과 석사
1995년 KAIST 전기및 전자공학과 박사
1999년 하이닉스(구 LG반도체) 연구소 책임연구원
1999년~현재 (주)옵토웨이퍼테크 연구소장
<주관심분야: 화합물반도체 광전 소자, GaAs-based VCSEL, PIN-PD, GaN LED, UV detector 소자 및 epitaxy, QD기술을 이용한 원적외선 광전소자>